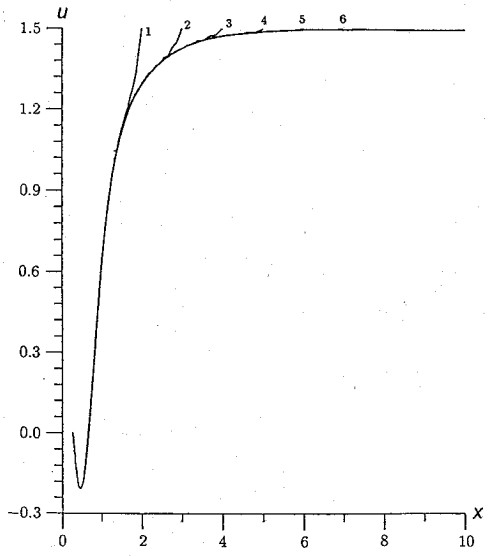


**Fig. 3 Comparison of the centerline velocity distribution for different upstream velocity distributions, $Re = 40$ and $x_d = 4.0$.**

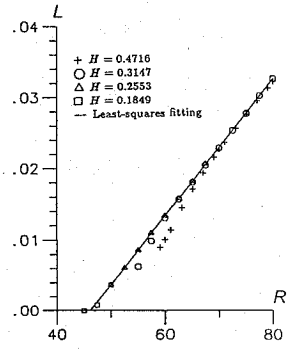


**Fig. 4 Estimate of $Re_r$ for $B = 0.1$, using meshes of different refinement; it is observed that a finer mesh is required for accurate simulation of a smaller recirculation region.**

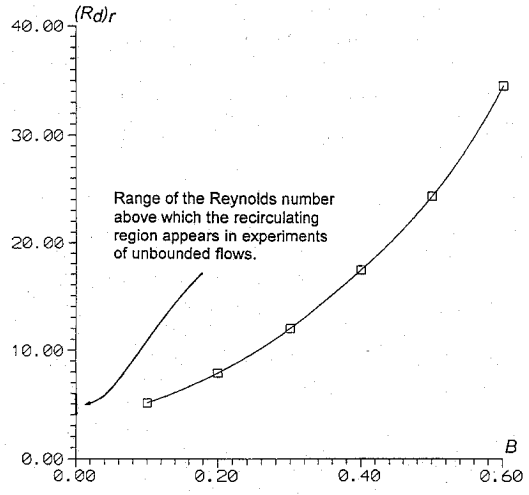


**Fig. 5 $(Re_d)_r$ for different blockage ratios.**

Furthermore, we define a new Reynolds number based on the diameter of the cylinder and the average speed of fluid flow at the cross section of $x = 0$,

$$Re_d := \frac{d(U_{\text{ave}})_{x=0}}{\nu} \tag{1}$$

Based on this definition, the value of $(Re_d)_r$, the Reynolds number above which the recirculation region appears, for different $B$ is shown in Fig. 5, together with an indication of possible range of $(Re_d)_r$ in an unbounded domain. According to the trend, the curve seems to converge to the same range as $B$ approaches zero.

## Concluding Remarks

The effects of the wall boundaries on the formation of the recirculating flow of the flow past a circular cylinder have been investigated. The computed data reveal that even at a small blockage ratio, such influence is still significant. This implies that care must be exercised when truncations of a flow domain is unavoidable for computational purposes. For a careful numerical study of the flow past a circular cylinder, it seems that the value of $B$ should not exceed 0.05, or even smaller.

In addition, it is also noticed that the uniform and parabolic velocity distribution at the upstream boundary do not lead to different centerline velocity profiles at the rear of the cylinder. Therefore, the upstream velocity distribution does not affect $Re_r$ because at this stage the Reynolds number is small and the viscous dissipation over the cylinder is strong.

## Acknowledgment

The author wishes to express his appreciation to the National Science Council of the Republic of China for the financial support of this work through Project NSC 80–0410-E-019-10.

## References

[1]Taneda, S., "Experimental Investigation of the Wakes Behind Cylinders and Plates at Low Reynolds, Numbers," *Journal of the Physical Society of Japan*, Vol. 11, No. 3, 1956, pp. 302–307.

[2]Fornberg, B., "Steady Viscous Flow past a Circular Cylinder up to Reynold Number 600," *Journal of Computational Physics*, Vol. 61, No. 2, 1985, pp. 297–320.

[3]Smith, F. T., "Laminar Flow of an Incompressible Fluid past a Bluff Body: The Separation, Reattachment, Eddy Properties and Drag," *Journal of Fluid Mechanics*, Vol. 92, 1979, pp. 171–205.

[4]Amick, C. J., "Properties of Steady Navier–Stokes Solutions for Certain Unbounded Channels and Pipes," *Nonlinear Analysis, Theory, Methods, and Applications*, Vol. 2, No. 6, 1978, pp. 689–720.

[5]Crouzeix, M., and Raviart, P.-A., "Conforming and Non-Conforming Finite Element Methods for Solving the Stationary Stokes Equations," *Revue Française d'Automatique Informatique et Recherche Opérationelle*, Vol. R-3, No. 1, 1973, pp. 33–76.

# Interaction of a Ribbon's Wake with a Turbulent Shear Flow

B. Chebbi* and S. Tavoularis†
*University of Ottawa,*
*Ottawa K1N 6N5, Ontario, Canada*

FOR nearly two decades, considerable attention has been given to thin ribbons or airfoils inserted in turbulent boundary layers (TBL) and their effects on the turbulence structure. Although the use of such devices for drag reduction does not appear very promising, their potential application in the reduction of noise, pressure fluctuations, and heat transfer still appears feasible. Recent investigations have attributed the observed decrease in skin friction to the reduction of the mean shear near the wall, caused by the ribbon's wake, and have demonstrated that small eddies generated in the wake attenuate the energy of the larger eddies and that the thin wake acts to isolate the inner and outer regions of the TBL. The structure of TBL is very complex. Besides producing the mean shear due to friction, the wall also imposes a kinematic constraint. Other influencing factors are turbulent transport and entrainment of the freestream fluid. Measurements in manipulated TBL are often of limited accuracy and hard to interpret, being frustrated by wall interference, severe requirements in spatial resolution, and wall curvature, as in flows

Received Feb. 25, 1994; revision received Aug. 18, 1994; accepted for publication Sept. 6, 1994. 

*Research Assistant, Department of Mechanical Engineering.
†Professor, Department of Mechanical Engineering.

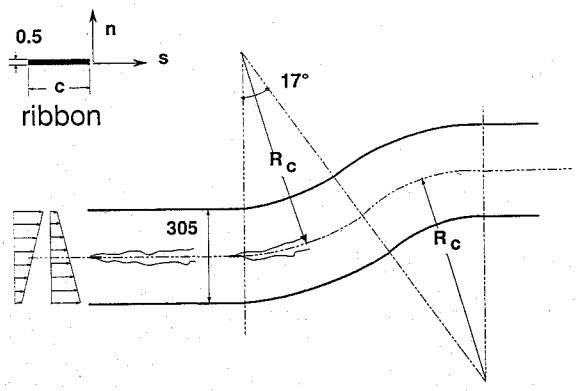


**Fig. 1 Sketch of the test section, indicating the locations of insertion of ribbon.**

over airfoils. Therefore, it seems worthwhile to study the interaction of a thin wake and a shear flow that is easily accessible and free from wall-related complications, although retaining a structure similar to that of TBL. The present investigation examines the wake of a thin ribbon in nearly homogeneous, uniformly sheared, turbulent flow, which is known to bear strong structural similarity to outer TBL.

The experimental facility, main features of the flow and measuring techniques have been described previously.[1,2] The flow was first led through a straight section, where it achieved a fully developed structure under the influence of uniform shearing and then it entered a curved section, consisting of two segments with opposite orientations of curvature but equal centerline radii, $R_c = 3500$ mm. The ribbon was inserted both in the straight and the curved sections (Fig. 1). Its width was $c = 12.5$ mm, comparable to the integral length scale in the flow, thus approximating the scaling of ribbons used in TBL studies.

Most measurements were taken with the ribbon positioned in rectilinear shear flow, at a distance of 1405 mm from the shear generator and aligned with the mean speed direction. The centerline speed $\overline{U}_{c0}$ was about 8.6 m/s, whereas the unmanipulated mean shear was about 54 $s^{-1}$. The turbulence attained a self-preserving structure in which all Reynolds stresses grew exponentially but their ratios remained constant.[1,2] Transverse profiles of the streamwise mean velocity, Reynolds stresses, and integral length scale across the wake are shown in Fig. 2, together with corresponding profiles in the absence of the ribbon. The mean velocity deficit in the wake became practically invisible beyond the streamwise distance $s/c = 32$, however, the ribbon's effects on the turbulent stresses persisted up to at least $s/c = 80$. Near the ribbon and toward the low-velocity side, there was a region where the local mean shear direction was opposite to the uniform mean shear direction and where the shear stress reversed sign. Farther downstream, the mean shear in the wake toward the low-velocity side remained lower than the uniform mean shear, thus resulting in lower local levels of turbulence production and creating a region of turbulent kinetic energy deficit. Toward the high-velocity side, the mean shear remained higher than the uniform mean shear, and the turbulence production and turbulent kinetic energy maintained local peaks, in excess of the unmanipulated levels, consistent with observations in TBL. The peaks became imperceptible beyond about $s/c = 32$, however, the regions of deficit were still apparent at $s/c = 80$. As in manipulated TBL, the wake spread more toward the low-velocity side, due to stronger diffusion at the lower velocities. The streamwise integral length scale and the Taylor microscale in the wake were lower than their unmanipulated values. The reduction in the integral length scales was visible up to the last measuring station ($s/c = 80$), whereas the Taylor microscales practically regained their freestream values beyond $s/c = 32$. Unlike TBL studies,[3] the present experiments show no tendency for $L_{uu}$ to reach or exceed the unmanipulated values at any stage in the wake development. A possible explanation for this difference is that those eddies which were forced to pass between the ribbon and the wall might have attained an elongated shape over some intermediate distance, beyond which they recovered their normal shape but at a statistically smaller size.

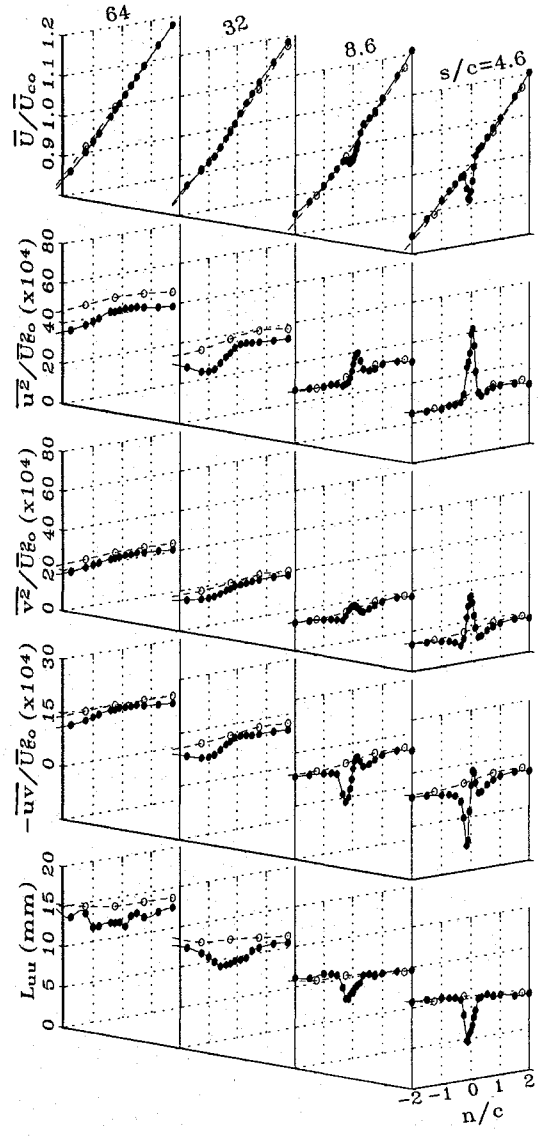


**Fig. 2 Profiles of turbulence properties across the wake (•) and in its absence (○) in rectilinear flow.**

Unlike statistical moments, spectral measurements can discriminate among different types of eddies possibly present in the flow. Samples of the one-dimensional frequency spectra, $F_{uu}$ and $F_{vv}$, of the streamwise and transverse velocity components and the coherence function $C_{uv}$ (real part only) are shown in Fig. 3. The spectral distortion in the wake was quite evident, especially for $F_{vv}$, which exhibited a strong peak. This peak was considerably attenuated at $s/c = 8.6$ and essentially disappeared at $s/c = 32$. In contrast, the attenuation of the large eddies persisted to the last measuring station, thus, documenting a permanent effect on these eddies. The spectra reveal the coexistence of two distinct types of eddies, apparently with distinct energy containing ranges: a set of larger eddies (to be referred to as freestream eddies), produced by the uniform mean shear and surviving to a certain degree in the wake, and a set of smaller eddies, produced by the velocity deficit in the wake. The reduction in the energy level of the large eddies could be attributed partly to their break up by the ribbon and partly to the enhanced viscous damping caused by the finer eddies in the ribbon's boundary layers and wake. It may also be deduced that the energy containing range of the wake-generated eddies overlaps with the inertial and viscous subranges of the freestream eddies, thus precluding the appearance of a universal equilibrium range. The explanation emerges now that peaks of normal stresses, observed in the near wake, are associated with the small eddies, which have a life time shorter than that of the large eddies, which are associated with the Reynolds stress deficit. These observations are in general agreement with spectral measurements in manipulated TBL.[4] In both types of flows, the size

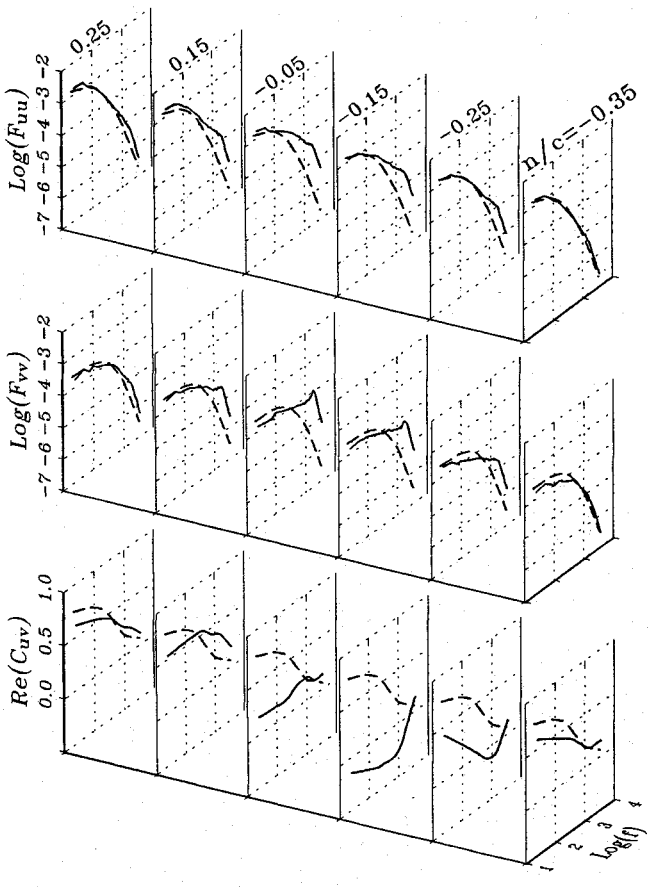


**Fig. 3 Frequency spectra and coherence function across the wake (—) and in its absence (- - -); rectilinear flow, $s/c = 4.6$.**

of the wake-generated, energy containing eddies, estimated from the frequency of the spectral peak and the local convection velocity, was comparable to the wake's width. The coherence function identifies regions of coexistence of two types of eddies with opposing shear stresses, not visible in the Reynolds stress profiles. For example, at $n/c = -0.25$, where the overall shear stress is nearly zero, there are large freestream eddies with negative shear stress and small wake-generated eddies with positive shear stress. In contrast, at $n/c = -0.05$, where the shear stress is also near zero, eddies of all sizes appear to be nearly uncorrelated. These observations can be easily explained by considering that the second location is at a local mean velocity maximum, at the edge of the wake, whereas the first location is at a local velocity minimum, at the center of the wake, and thus more likely to contain wake-produced eddies than the former case is. Furthermore, examination of the coherence at $n/c = -0.35$ and 0.015, which lie on the opposite edges of the wake, reveals that they have comparable correlation coefficients, but different eddy structures. At the latter location, which is on the high-velocity side of the wake, the small, wake-generated eddies have considerably higher values of shear stress.

An issue of concern in TBL studies has been the effect of ribbon inclination. Present measurements with the ribbon inclined at positive and negative angles of ±3 deg showed this effect to be quite weak, with the shear stress exhibiting the highest sensitivity; at positive inclination the minimum shear stress was slightly larger than that at no inclination and its location was shifted towards the low-velocity side, whereas negative inclination caused the opposite effects. One may reconcile the present results with TBL measurements,[5] showing that small positive inclination would increase the reduction of wall shear stress, by the conjecture that in proximity of a wall streamline displacement toward the wall would cause the wake to approach the wall at a closer downstream distance, where its effect would be stronger. Another issue of practical interest is the effect of a curved boundary. This effect was assessed by placing the ribbon in curved sections, corresponding to both convex and concave boundary layers, depending on whether the curvature parameter $S = (\overline{U}_{c0}/R_c)/(\partial\overline{U}/\partial n)$, was positive or negative.[2] In all cases, $|S| \approx 0.05$. The turbulence structure in the wake was found to be essentially unaffected by curvature, which implies that eddies produced by the wake are sufficiently small to follow the mean streamlines without substantial distortion by centrifugal actions. On the other hand, the wake axis was consistently shifting toward the center of curvature, because centrifugal actions tend to divert slower fluid toward the center and faster fluid away from it. This result leads to the speculation that the wake of a ribbon over a convex wall would tend to shift closer to the wall than that over a plane wall, thus causing a larger wall shear stress reduction; the reverse would happen over a concave wall.

The present types of wakes do not admit a self-similar solution, because of the freestream nonuniformity and the streamwise change in the outer turbulence. Nevertheless, an empirical decay law was sought by plotting the maximum velocity deficit vs $s$ for the present measurements as well as for manipulated TBL. The results were compatible with a power decay law, with an average decay exponent of −0.67, which is measurably larger than the typical value of −0.5 for wakes in low-turbulence, uniform flows, but closer to the value −0.62 for wakes in grid-generated turbulence. All sets of measurements approximately collapsed when nondimensionalized by the estimated momentum thickness of the boundary layer over the ribbon. The spreading rate of the wake could be approximated by a power law with an average exponent of 0.53.

Finally, the applicability of gradient transport to the present configuration was also tested. As shown in Fig. 4a, the data form a

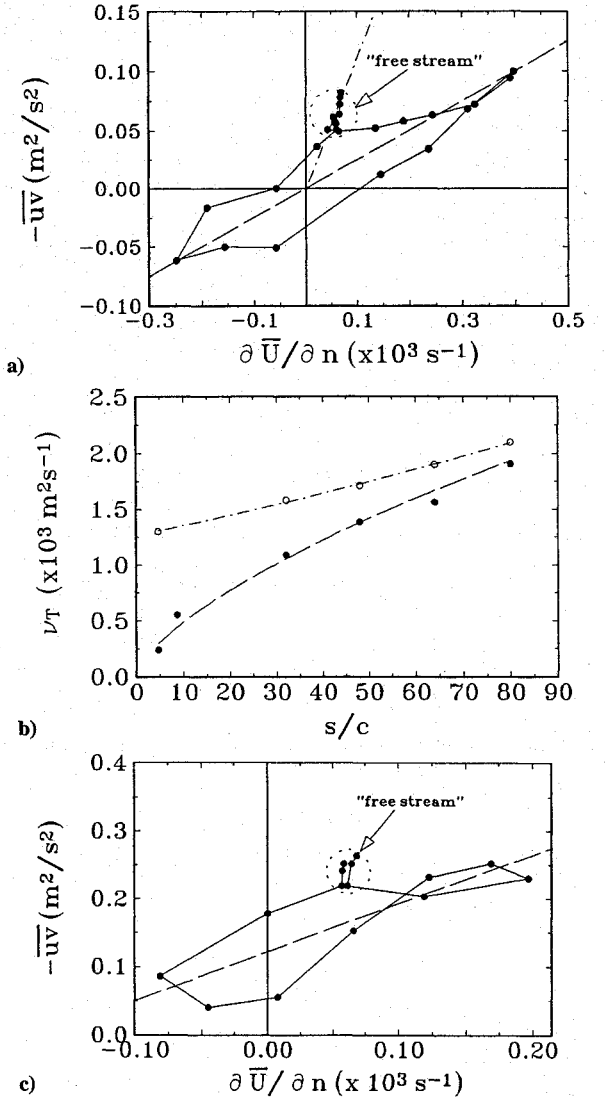


**Fig. 4 Estimates of the overall eddy viscosity across the wake in a) and b) rectilinear flow and c) curved flow, $S = -0.05$.**

loop, which starts at the freestream toward the low-velocity side, closes again toward the high-velocity side and contains two regions of countergradient transport (i.e., where $\partial\overline{U}/\partial n$ and $-\overline{uv}$ are of opposite signs). In the near wake, where the mean shear has regions of opposite signs, the loop extends over all four quadrants, but, farther downstream, it shrinks within the same quadrant as the freestream points. Despite its apparent local failure, gradient transport seems appropriate for a global description of the wake, if the loop is approximated by a straight line passing through the origin. The slope of this line, corresponding to the average eddy viscosity in the wake, was considerably lower than that in the outer flow, although their difference decreased with streamwise distance (Fig. 4b). By contrast to the rectilinear flow, gradient transport failed locally as well as globally to describe the thin wake in the curved flow (Fig. 4c), where the mean line through the data loops could not be made to pass through the origin. This is not so much an effect of the wake, but a general limitation of this concept in curved flows.

## References

[1]Tavoularis, S., and Karnik, U., "Further Experiments on the Evolution of Turbulent Stresses and Scales in Uniformly Sheared Turbulence," *Journal of Fluid Mechanics*, Vol. 20, 1989, pp. 457–478.

[2]Holloway, A. G. L., and Tavoularis, S., "The Effects of Curvature on Sheared Turbulence," *Journal of Fluid Mechanics*, Vol. 237, 1992, pp. 569–603.

[3]Blackwelder, R. F., and Chang, S. I., "Length Scales and Correlations in a LEBU Modifided Turbulent Boundary Layer," AIAA Paper 86-0287, 1986.

[4]Bonnet, J. P., Delville, J., and Lemay, J., "Study of LEBUs in Modified Turbulent Boundary Layer by Use of Passive Temperature Contamination," Proceedings of the Symposium on Turbulent Drag Reduction by Passive Means, Royal Aeronautical Society, 1987.

[5]Bandyopadhyay, P. R., and Watson, R. D., "Pressure Field due to Drag Reducing Outer Layer Devices in Turbulent Boundary Layers," *Experiments in Fluids*, Vol. 5, 1987, pp. 393–400.

# Subsonic Boundary-Layer Tripping by Strip Blowing

J. A. Masad* and R. Abid†
*High Technology Corporation, Hampton, Virginia 23666*
and
A. S. Abdelnaser‡
*Virginia Polytechnic Institute and State University, Blacksburg, Virginia 24061*

THE achievement of earlier transition by artificial tripping of the boundary layer is often desired in wind-tunnel operations to simulate turbulent boundary-layer behavior at full-scale Reynolds numbers. The most common method for tripping the boundary layer is the use of roughness. The existence of roughness enhances the instability of the flow and accelerates the onset of transition and, consequently, the occurrence of turbulence. This approach to tripping the boundary layer with roughness elements becomes more difficult at higher speeds. A major difficulty associated with the use of roughness is that it can cause flow separation and can lead to global breakaway of the flow and vortex shedding, which prevent the formation of a "clean" attached turbulent boundary layer. For this reason, research into alternate techniques for tripping the boundary layer that may avoid the difficulties associated with the use of roughness is necessary.

Received Dec. 2, 1994; revision received Feb. 6, 1995; accepted for publication Feb. 7, 1995. 

*Research Scientist, 28 Research Drive. Senior Member AIAA.

†Senior Research Scientist, 28 Research Drive. Member AIAA.

‡Visiting Assistant Professor, Department of Engineering Science and Mechanics. Member AIAA.

The occurrence of laminar separation on aerodynamic surfaces increases pressure drag and reduces lift, which results in a reduction in the efficiency of these surfaces. Separation can result from a localized adverse pressure gradient created by surface roughness,[1] or it can result from extended regions of adverse pressure gradient due to the curvature of the surface. In both cases, the flow may separate while it is still laminar. Masad and Malik[2] showed that at certain conditions the location of transition onset is further downstream of the location of the onset of separation. This phenomenon is particularly true at low unit Reynolds numbers, at increasing Mach numbers, or in the presence of a short roughness element. In situations in which laminar separation is about to occur, tripping the boundary layer so that it remains attached is preferable. Transition causes the point of separation to move downstream because in a turbulent boundary layer the accelerating influence of the external flow extends farther due to turbulent mixing. In turn, the dead area decreases considerably, which reduces the pressure drag. These phenomena are the second reason for studying alternative techniques for tripping the boundary layer. In this work, we study the effect of using strip blowing on the location of transition onset in subsonic flow over a flat plate. We use linear stability theory, coupled with the empirical $e^N$ method, to predict the transition onset location.

We consider a two-dimensional subsonic flow over a flat plate in the presence of discrete blowing. As a result of the discrete blowing, both a viscous-inviscid interaction and an upstream influence exist, and we use the interacting boundary layer (IBL) theory to analyze the flowfield (see Davis[3]). Extensive details of the IBL formulation for two-dimensional subsonic flow are given by Nayfeh and Abu Khajeel (see Abu Khajeel[4]). In cases with suction or blowing, the velocity of the flow through the surface is denoted by $v_w$ and is made nondimensional with respect to the freestream streamwise velocity $U^*_\infty$. For suction, $v_w$ is negative; for blowing, $v_w$ is positive. The length of the suction or blowing strip is denoted by $\lambda$.

In stability analysis, small, unsteady two-dimensional disturbances are superimposed on the mean-flow quantities, which are computed with the IBL theory. Mack[5] showed that the most amplified waves in two-dimensional flow with a freestream Mach number $M_\infty$ of less than approximately 0.8 are two-dimensional waves. Next, the total quantities are substituted into the Navier–Stokes (NS) equations, the equations for the basic state are subtracted out, the quasiparallel assumption is invoked, and the equations are linearized with respect to the disturbance quantities. The disturbance quantities are assumed to have the normal-mode form, so that a disturbance quantity $\hat{q}$ is

$$\hat{q} = \xi(y) \exp i(\alpha x - \omega t) + \text{complex conjugate} \tag{1}$$

The streamwise coordinate is $x$, $t$ is the time, and $\alpha$ and $\omega$ are generally complex. In the stability analysis and the computations throughout this work, the reference length is $\delta^*_r = \sqrt{\nu^*_\infty x^*/U^*_\infty}$, the reference velocity is $U^*_\infty$, the reference time is $\delta^*_r/U^*_\infty$, the reference temperature is the freestream temperature $T^*_\infty$, the reference viscosity is the freestream dynamic viscosity $\mu^*_\infty$, and the pressure is made nondimensional with respect to $\rho^*_\infty U^{*2}_\infty$ (where $\rho^*_\infty$ is the freestream density). The viscosity varies with temperature in accordance with Sutherland's formula; the specific heat at constant pressure $C^*_p$ is constant, and the Prandtl number $Pr$ is constant and equal to 0.72. For the spatial stability of the two-dimensional flow considered in this work, $\omega$ is real, and $\alpha$ is complex, where the real part $\alpha_r$ is the streamwise wave number and the negative of the imaginary part $-\alpha_i$ is the spatial growth rate. The frequency $\omega$ is related to the dimensional circular frequency $\omega^*$ through $\omega = \omega^*\delta^*_r/U^*_\infty$, which leads (with the definition of $\delta^*_r$) to

$$\omega = FR \tag{2}$$

where

$$F = \frac{\omega^* \nu^*_\infty}{U^{*2}_\infty} \tag{3}$$

and

$$R = U^*_\infty \delta^*_r/\nu^*_\infty = \sqrt{xRe} = \sqrt{Re_x} \tag{4}$$